Development of a beam-based phase feed-forward demonstration at the CLIC Test Facility (CTF3).

Jack Roberts
New College, Oxford

Thesis submitted in fulfilment of the requirements for the degree of Doctor of Philosophy at the University of Oxford

Trinity Term, 2016

Abstract

This is the abstract TeX for the thesis and the stand-alone abstract.

Dedication.

Acknowledgements

Acknowledgements.

Contents

List of Figures

List of Tables

Glossary

Item1 Description.

Item2 Description.

Item3 Description.

Chapter 1

Setup and Commissioning of the PFF System

This is the introductory text.

1.1 Feedforward Controller (FONT5a Board)

1.1.1 Cabling Setup

1.1.2 Implementation of PFF Algorithm in Firmware

Not using arcsin in phase reconstruction - effect

Gain conversion factor

1.1.3 DAQ and Setup Parameters

gain

filter weights

timing delays

saturate rather than overflow output

Interleaved mode

1.1.4 ADC Droop Correction

The droop in the response of the FONT5 ADCs, as most clearly seen in the output of the diode channel in Figure 1.1 (although it also effects the mixer channel), is not an issue for the work the FONT group does at ATF2 where the signals are well approximated by
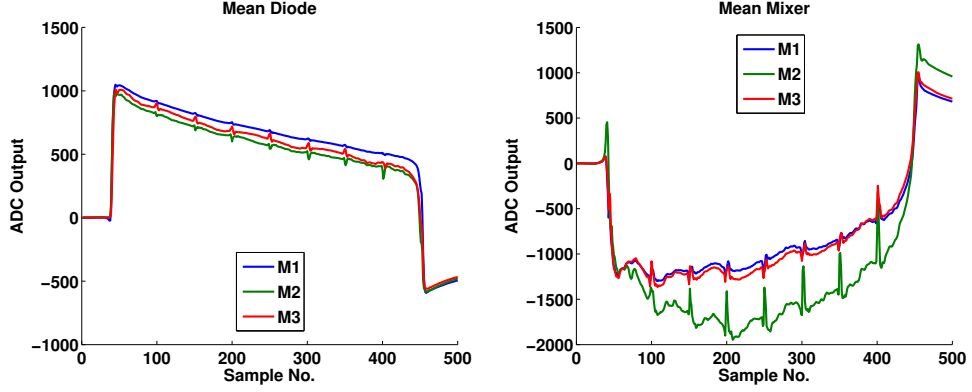
1

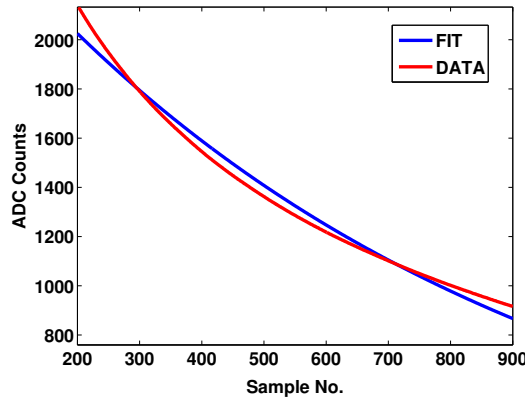Figure 1.1: Mean diode and mixer output with no filter.

Figure 1.2: Attempted exponential fit to the ADC droop.

delta functions separated by $\sim$100 ns. Although the droop has been seen previously, its significance for the continuous microsecond length pulse at CTF3 had not been considered because of this.

The droop emerges as a result of the use of AC coupling on the ADC input transformers for electrical isolation. This involves using a capacitor, the current across which is dependent on dV/dt (V being voltage and t time), to remove the DC component from a signal. In particular for the diode channel, which should be a square wave, the output is increasingly well described by a DC signal on the flat top as you move away from the leading edge of the pulse, with the capacitor causing droop in the response as a result.

In the simplest case the droop should be well described by an exponential decay of the form $A \exp(-t/T)$. The droop makes it difficult to perform calibrations and measurements on the data and one way in which it could be removed in offline analysis is by determining the decay constants, T, for each of the ADCs on the FONT5 board. To avoid the influence of beam effects tests were done in Oxford using a generated 10 μs DC pulse.

Unfortunately, as can be seen in Figure 1.2 which shows an example of an exponential fit for one ADC, although the fits return good R^2 values it is clear that the slope of the exponential curve is not a good match for the slope of the data. This is perhaps not unexpected as the ferrite cores used in the transformers have many non-linear properties. In fact, by

using a fit with two exponential terms it is possible to obtain a perfect match to the data but at this point the complexity of the fit would make any attempt to remove the droop in real beam data in this way spurious.

Instead, changes will be made to the currently in development FONT5a board hardware and firmware to greatly reduce the scale of the droop. Different transformers will be used to reduce the droop rate by up to a factor of fifty and in addition digital filtering will be implemented in firmware to smooth out and reduce the remaining droop component even further. It is expected that after these changes the droop will be small enough to not have a detrimental effect on the performance of the phase feedforward system.

1.2   Amplifier

Make point that all effects here much smaller than phase monitors/phase propagation and although important to highlight them no attempts yet made to correct them or take them in to account in simulations.

Amplifier versions:

First version (nov 2014) 350 V (check)

2nd version (jul 2015) 650 V - double FETs

3rd version: 1200 V with combiner module (?) not pursued

1.2.1   Installation

Amplifier inputs:

Trigger from FONT5a board

DAC1 and DAC2 from FONT5a board

Amplifier outputs:

4 drive signals - one for each strip. Sent to downstream end of kicker (why?)

4 terminators

Amplifier on time monitoring

Monitoring of each amplifier output

1.2.2   Linearity

Figure 1.4 shows the amplifier output, as measured by the monitoring signals, at different constant input voltages sent from the FONT5a board between the minimum of -2V (-4096 DAC counts) and maximum of 2V (+4096 DAC counts). The output voltage from the
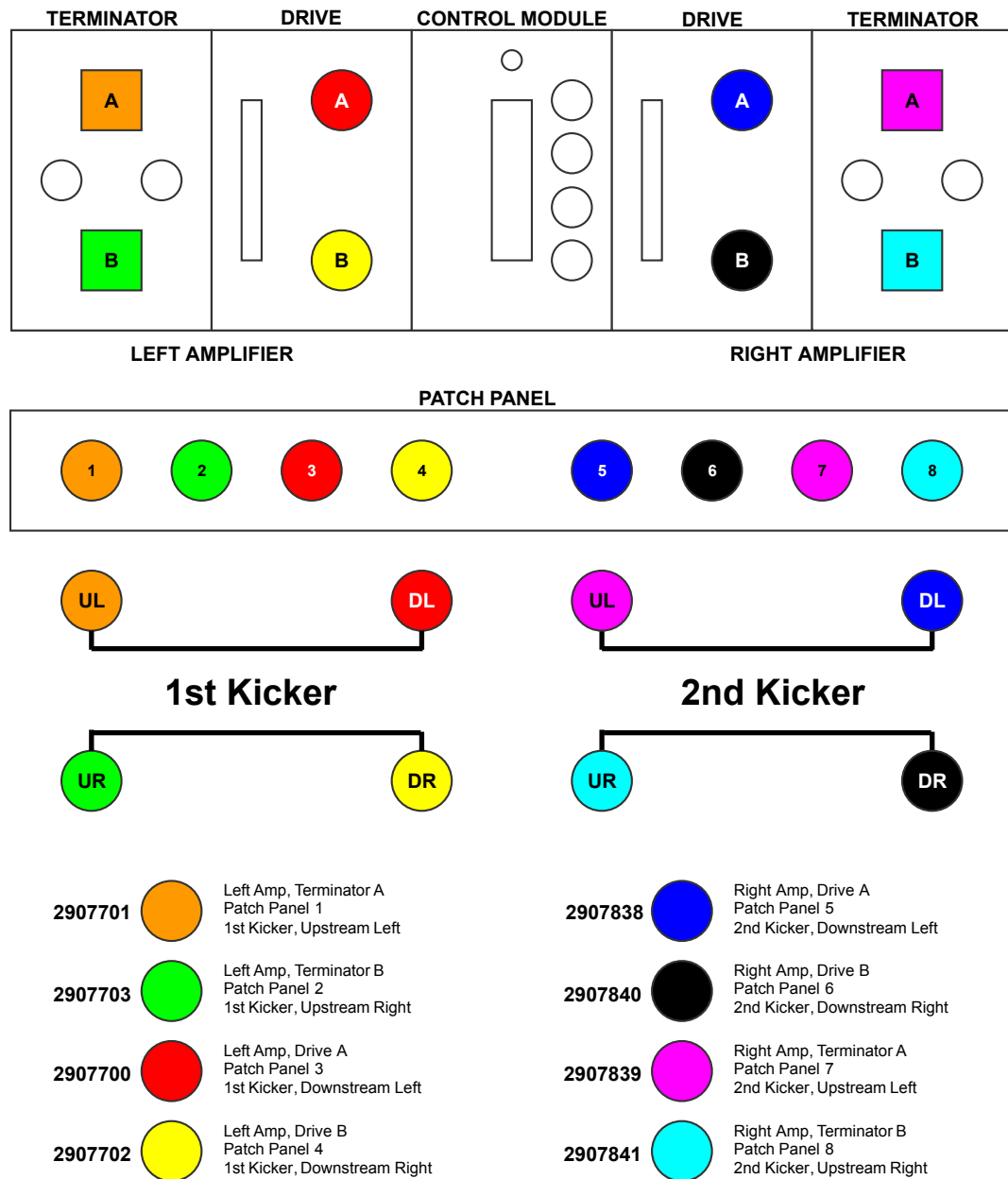
Figure 1.3: Cabling setup for cables between the amplifier and kickers.

monitoring signals is converted in to the real amplifier output Voltage using the approximate conversion factor of 115. All four amplifier outputs are shown (one for each strip of the two kickers). The plotted values are means taken across a 480 ns central part of the whole 1400 ns output pulse.

The relative polarity of the four outputs is equivalent to what would be sent to the kickers during PFF operation, with opposite polarity of the L and R amplifier outputs sent to each kicker, so that the beam is kicked in opposite directions by each kicker with the second kicker then closing the orbit bump created by the first. Within each side of the amplifier the A and B outputs (sent to each side of the kicker) also have opposite polarity, necessary to create the potential difference across the strips within each kicker that creates the deflecting field for the beam. The relative polarity of the A and B outputs is fixed in the amplifier design and cannot be controlled via the FONT5a board.

The response of the amplifier is highly linear in the region between ± 1.2 V sent to the amplifier. Outside this range the amplifier clearly begins to enter saturation, in particular above input voltages of ± 1.7 V. The linear fits shown include only the points between ± 1.2 V, excluding the first and last three points in the scan of input voltages, in order to not be biased by the effects of saturation.

Figure 1.5 shows the residuals between the linear fit and the real amplifier output across the full range of input voltages. By looking at the residuals a slight deviation from linearity in the ± 1.2 V range is also visible, although the maximum difference is only 10 V or a 3% relative error. At the maximum input voltage of ± 2 V the difference between the real output and the amplitude expected if the response was linear across the full range rises above 150 V, or a relative error of more than 25%. For example, the RB output at an input voltage of $+2$ V is 605 V but the fitted response gives 769 V, a difference of 164 V or 27%.

The effects of amplifier saturation are not taken in to account in the PFF algorithm on the FONT5a board, in which the DAC output is linearly dependent on the input phase (voltage from the phase monitor mixer signal) across the full range. The applied correction to the downstream phase will therefore be non-optimal when the DAC output calculated by the PFF algorithm is above an absolute value of 2500 counts (1.2 V sent to the amplifier). To date the non-linearity of the amplifier as it begins to enter saturation has also not been included in the PFF simulations presented in the following chapters. This may partially explain the small discrepancies seen between the simulated and real results in some datasets, so including the effect will be pursued in the future. In addition, it could be foreseen to incorporate the saturation characteristics in to the PFF algorithm on the FONT5a board, so that calculated outputs above 2500 counts are boosted slightly to compensate for the lower than expected amplifier output.

Discrepancies between the four amplifier outputs are also visible in Figure 1.5 and Table 1.1, both in terms of gradient and peak output. This can be partially but not completely explained by errors of up to a few percent in the precise calibration of the four monitoring outputs, which do not output exactly 1/115 of the real input voltage [TODO: Ask Colin about errors]. Differences between the A and B outputs sent to each kicker are not an issue for the PFF performance as both are linear (in the ± 1.2 V range) and the kick experienced
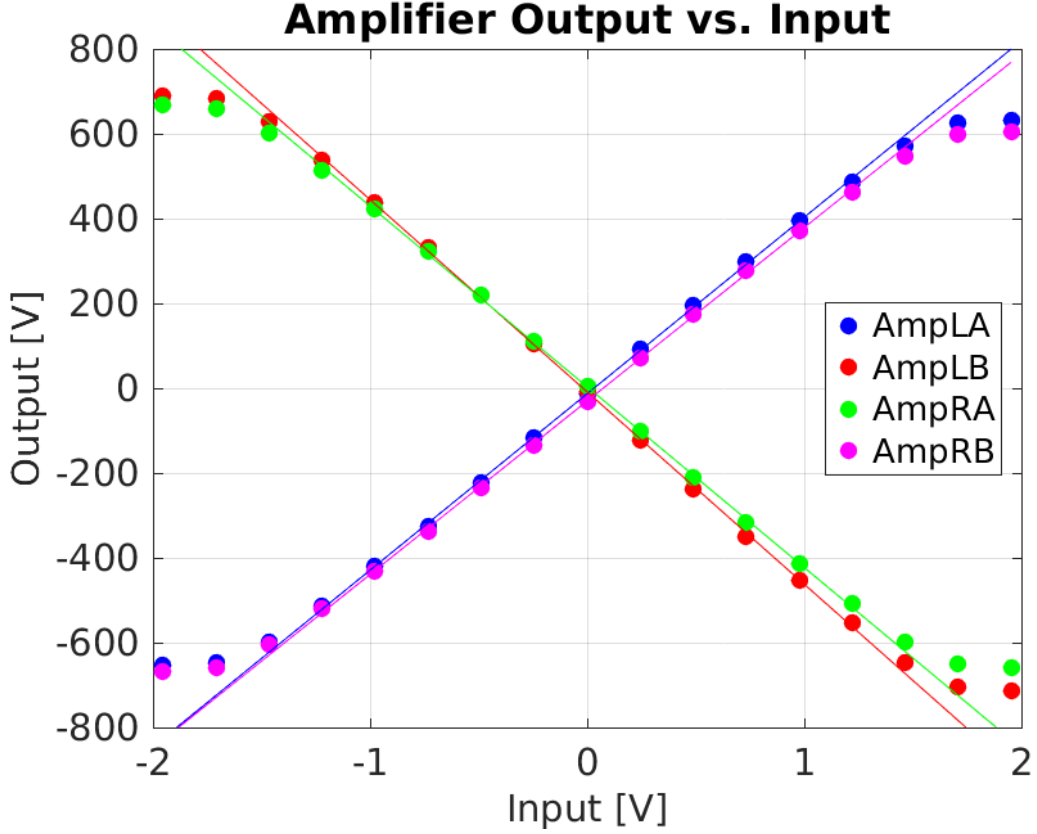
Figure 1.4: Amplifier output vs. input.

Amplifier Port	Output at +1 V Input
LA	$+416 \pm 3$ V
LB	-453 ± 3 V
RA	-426 ± 3 V
RB	$+409 \pm 3$ V

Table 1.1: Feedforward results using combined data from 20th November 2015.

by the beam in each kicker is proportional to the difference of the two. Therefore, only the calibration between the output from the FONT5a board sent to the amplifier and the resulting phase shift in the TL2 chicane is affected. However, disparity between the potential difference across each kicker (LA-LB and RA-RB), so that the deflection of the beam in each kicker is different, leads to the orbit bump created by the PFF system not being closed in the chicane, degrading the horizontal beam stability downstream. The fitted potential difference at 1 V input is 869 V for the left amplifier (LA-LB, sent to the first kicker) and 835 V for the right amplifier (RA-RB, sent to the second kicker), a difference of 4%. This can be compensated in the PFF setup on the FONT5a board by using a different gain for each correction output, so that the voltage sent to the right amplifier is higher but the resulting output voltage sent to both kickers is the same. Orbit closure is discussed further in Section 1.5.3.
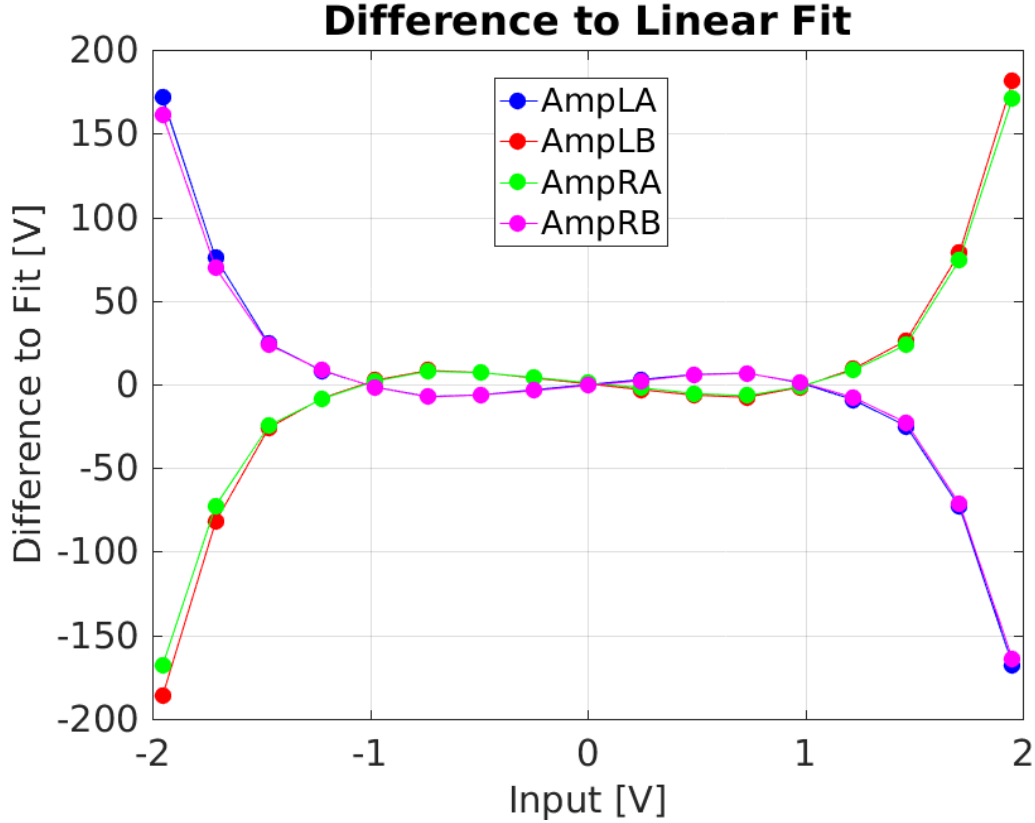
Figure 1.5: Residual between amplifier output and linear fit.

1.2.3   Shape

In the previous section the linearity of the mean output was considered but the performance of the PFF correction is clearly also sensitive to any variations in output voltage along the amplifier output pulse. Figures 1.6 and 1.7 show the full 1.4 μs amplifier output pulse at a constant $+1$ V input sent to the left amplifier and a constant -1 V input sent to the right amplifier respectively. Spikes in the signal just prior to 2000 ns and after 3000 ns on the time axis as seen in the plots are beam pickup induced by the beam passing through the kickers. These are therefore not a property of the amplifier performance and are excluded from the analysis in this section. However, the beam pickup is used later in Section 1.6.1 for the purposes of optimising the correction timing.

For each side of the amplifier both the A and B outputs are plotted as well as the difference of the two, which is the relevant quantity in terms of the kick received by the beam as it traverses the kickers. In the ideal case the potential difference should be flat along the full pulse length. However, for both the left and right side variations in the difference are visible, with an initial increase in output across the first 500 ns of the pulse followed by a droop in response across the second half of the pulse. Although not shown here, the shape of the variations along the pulse is consistent across the full range of output voltages, and scale in magnitude with the output voltage. Figure 1.8 shows the peak-to-peak and mean deviation of the output voltage along the pulse across the full range of input voltages. The peak-to-peak deviation refers to the difference between the minimum and maximum output along
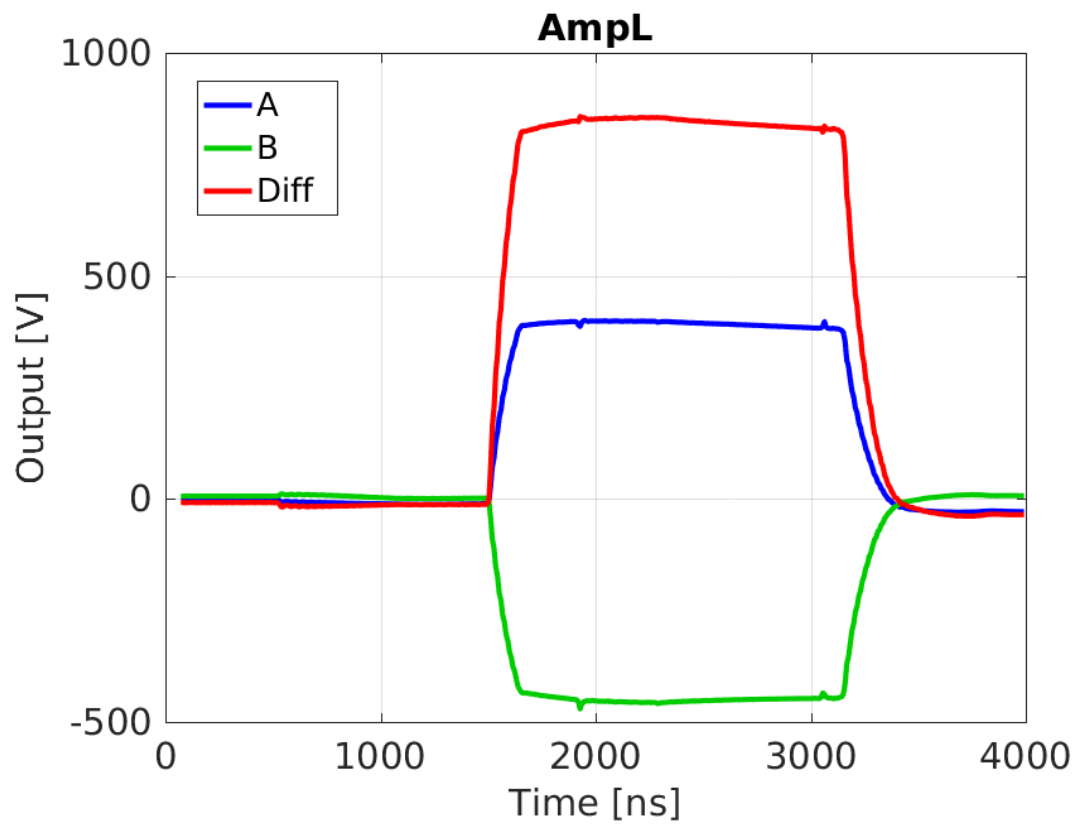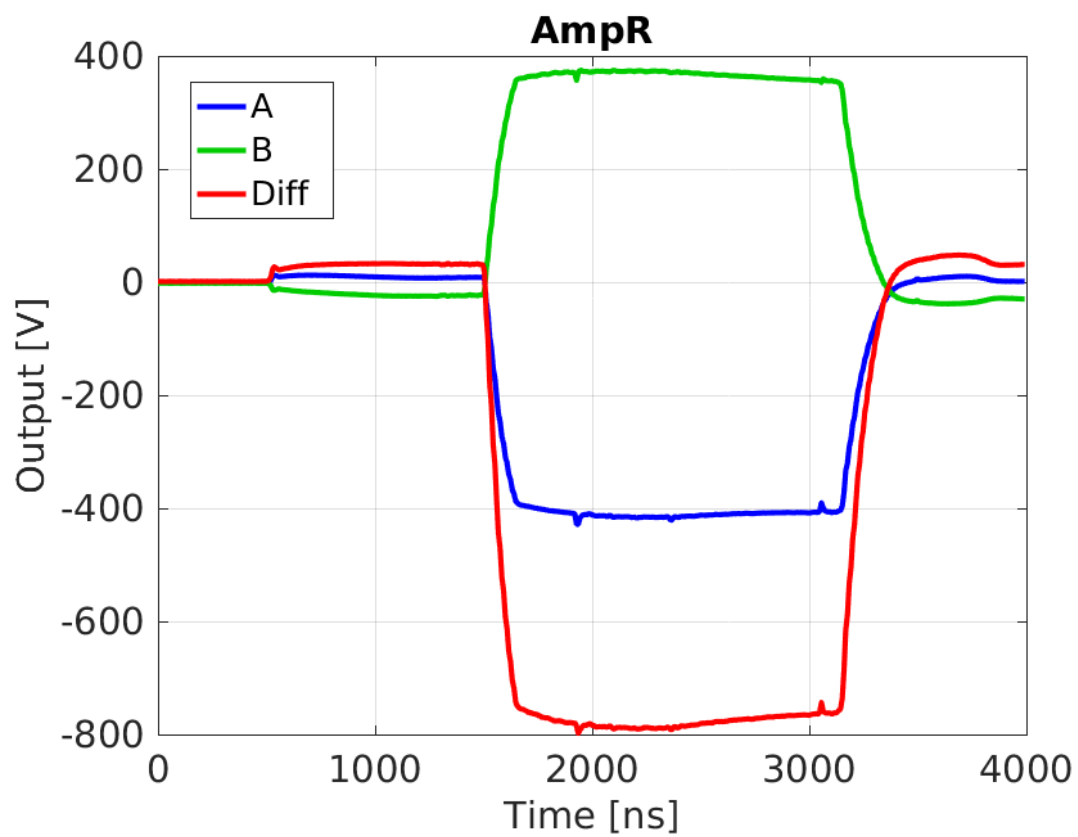
Figure 1.6: Amp L along pulse at 1 V input

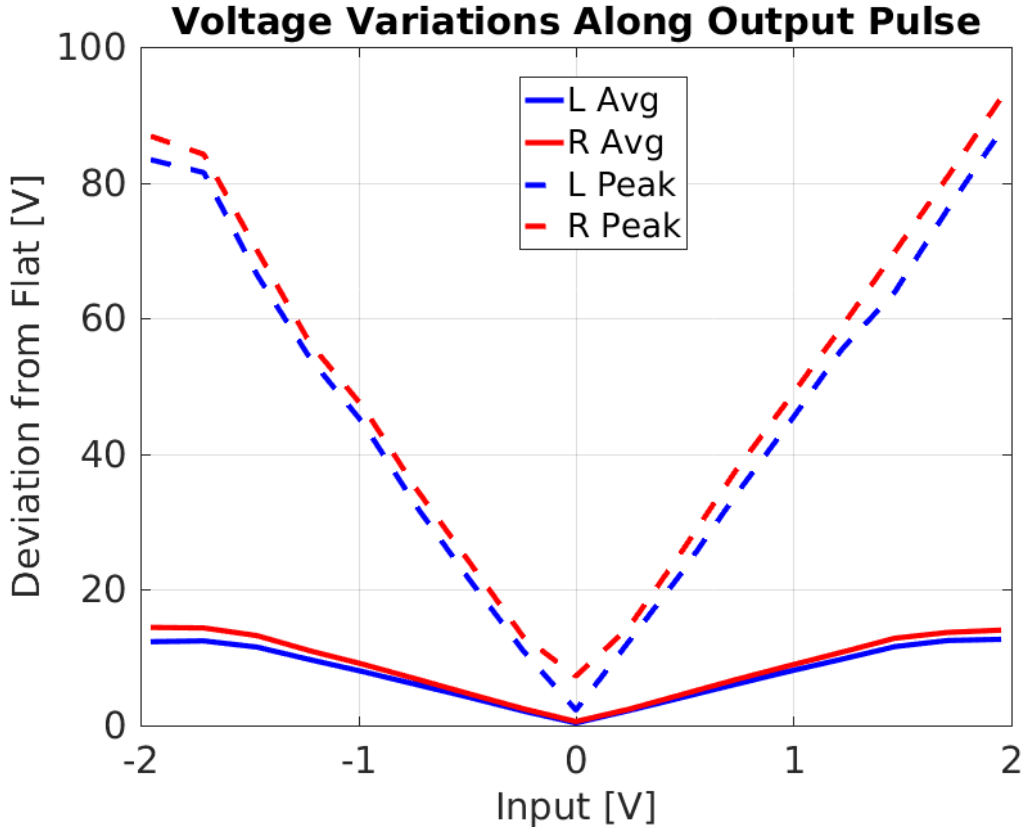Figure 1.7: Amp R along pulse at 1 V input

Figure 1.8: Flatness of potential difference sent to kickers.

the pulse, whilst the mean deviation is the average absolute difference between the mean output and the output at each sample point. For a constant input voltage the output voltage along the pulse varies by up to 88 V peak-to-peak (mean 12 V) for the left amplifier or 93 V peak-to-peak (mean 14 V) for the right amplifier. As a relative difference, this corresponds to approximately a 6 % peak-to-peak, or 1 % mean, variation along the pulse.

The PFF algorithm on the FONT5a board uses a single gain value across the whole pulse length for each correction output, thus making the approximation that the amplifier response is flat along the pulse. The variations along the amplifier pulse therefore directly translate in to discrepancies between the intended phase shift as calculated and the real phase shift experienced by the beam. As the region of interest for the correction is a few hundred nanoseconds about the central part of the pulse, as opposed to the full pulse length, the 1 % mean variation is more indicative of the resulting error than the 6 % peak-to-peak variation. With a correction range (Section 1.5.1) of $\pm6°$, the effects of the non-flat amplifier output should be below $0.06°$ and not measurable considering the phase monitor resolution of $0.14°$. Nevertheless, it could be foreseen to implement a droop correction in the PFF algorithm on the FONT5a board, taking the variations in the amplifier output along the pulse in to account.

As for the mean output voltage, the second way variations in the amplifier output along the pulse can impact the PFF performance is via the orbit closure in the chicane. For this the relevant quantity is the sum of the potential difference sent to each kicker, or
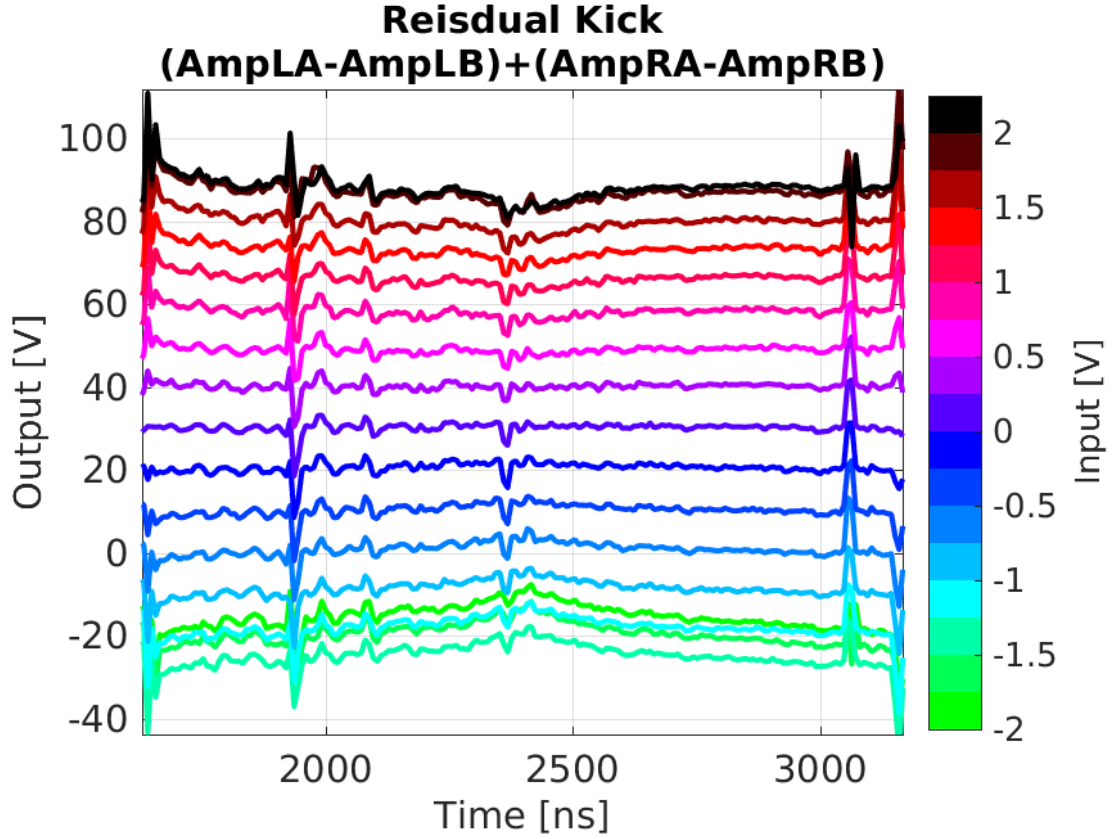
Figure 1.9: Residual kick along pulse.

$(LA - LB) + (RA - RB)$. To ensure orbit closure this quantity, named the residual kick here, should be zero across the whole pulse length for all input voltages. Figure 1.9 shows the residual kick along the pulse for all the input voltages in the scan. Clearly they are not all centred around zero, but this is expected due to the differences in the mean output voltage of the four amplifier outputs seen in the previous section. As already stated, the overall mean offset can be removed by using a different gain for the two correction outputs. However, any variations along the pulse cannot be compensated for in the PFF algorithm. The magnitude of the effect is summarised in Figure 1.10, showing the peak-to-peak and average deviation of the residual kick from flat. The overall residual kick is very flat and effect is smaller than any of those previously shown — only up to 2 V on the mean or 21 V peak-to-peak. Whether this has any measurable effect on the orbit closure is discussed in Section 1.5.3.

1.2.4 Bandwidth

1.3 Data Acquisition and Signal Processing

1.3.1 SiS Digitiser Setup

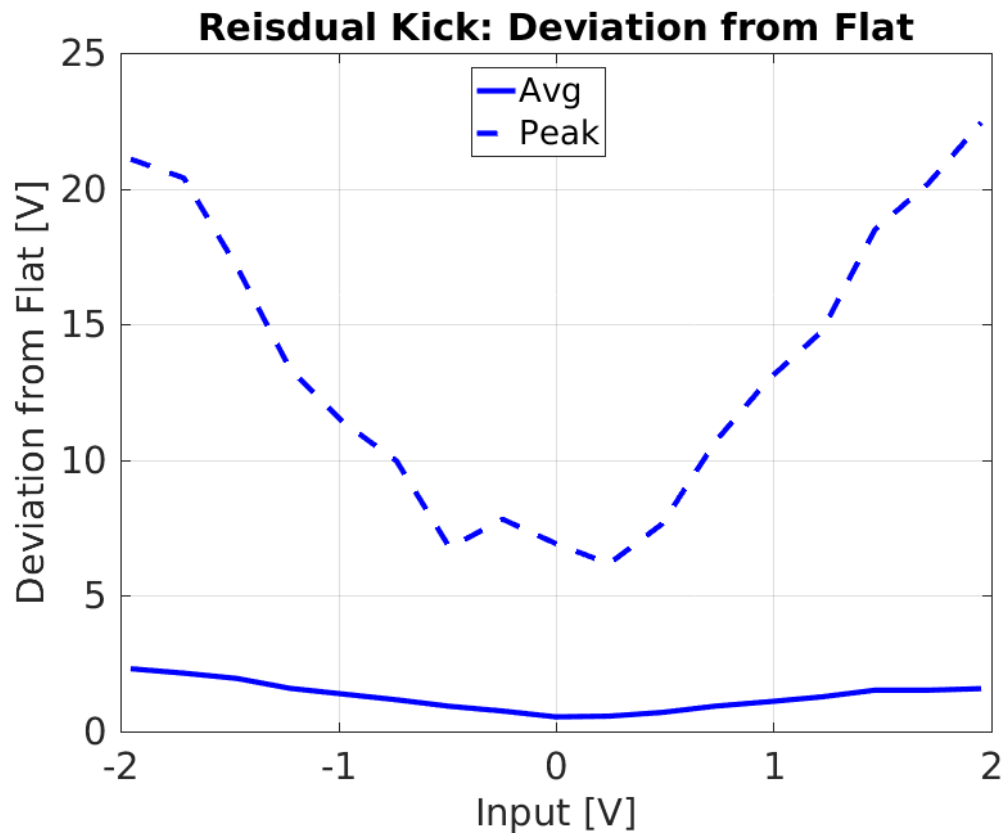(already discussed in ph mon chapter)

Figure 1.10: Residual kick along pulse: deviation from flat.

1.3.2   Acquisition Tools

1.3.3   Monitoring Tools

Online display

1.3.4   Time Alignment of Signals

1.3.5   Definition of Zero Phase

1.4   Latency

Kicker pick-up theory Kicker why drive downstream end theory Cable length measurements (cutting, matching length of drive pairs)

	Phase Shift at +1 V Input	Max Phase Shift
Data	$3.5 \pm 0.1°$	$5.5 \pm 0.3°$
Model	$3.6°$	$5.6°$

Table 1.2: Phase shift at +1 volt input to the amplifier.

1.5 Kicker and Optics Performance Verification

1.5.1 Correction Range

Knowledge of the correction range of the PFF system, or more specifically the relationship between the voltage sent to the amplifier and the phase shift in the chicane, is critical for the PFF setup. The first checks of the ability to shift the phase in the TL2 chicane using the new phase feedforward optics were performed with magnetic correctors prior to the PFF amplifier being available (these correctors can be used to implement a secondary "Slow Correction" to complement the PFF system, as discussed in Section **??**). Aside from their use for the PFF correction, these tests and the clear variation with beam phase versus voltage sent to the PFF kickers shown in this section are already a significant achievement and a verification of the extensive work to improve the MADX model of TL2 presented in Chapter **??**.

Figure 1.11 shows the mean phase shift after the chicane (in the downstream phase monitor) across the full ± 2 V input range of the amplifier. Constant DAC outputs from the FONT5a board were sent to the amplifier in 17 steps between -4096 counts (-2 V) and +4096 counts (+2 V). In order to reduce the sensitivity to any drifts in the beam phase between data points the scan was taken in interleaved mode, alternating between pulses with no drive sent to the amplifier and a constant non-zero DAC output. The phase plotted in Figure 1.11 is therefore the difference between 50 kicked beam pulses and 50 "nominal" pulses taken at the same time for each amplifier input voltage.

At the maximum amplifier input voltage of 2 V the phase after the chicane is shifted by $5.5 \pm 0.3°$. The fitted phase shift per Volt sent to the amplifier is $3.5 \pm 0.1°$ in the ± 1.2 V linear range of the amplifier (excluding the first and last three points, blue "FIT" line in Figure 1.11). This fitted gradient is required and was previously introduced for the conversion between the PFF gain in the units on the FONT5a board and the real applied gain in Section 1.1.2. In Section 1.1.2 it was quoted in terms of the phase shift in radians per DAC count output from the FONT5a board, rather than degrees per Volt as shown here. The value of 30μrad/count is easily derived using the conversion factors between degrees and radians and knowing that a DAC output of 4096 counts corresponds to 2 V sent to the amplifier. [TODO: Calculated factor is 29.827 microradians/count here. One I actually used for gain conversion, simulations etc. was 26.18 (used full range rather than linear range)]

Given knowledge of the amplifier output characteristics (Section 1.2.2), the kicker specifications (Section **??**) and the chicane optics (Section **??**) the real phase shift seen in the scan can be compared to the expected phase shift based on the system parameters. The
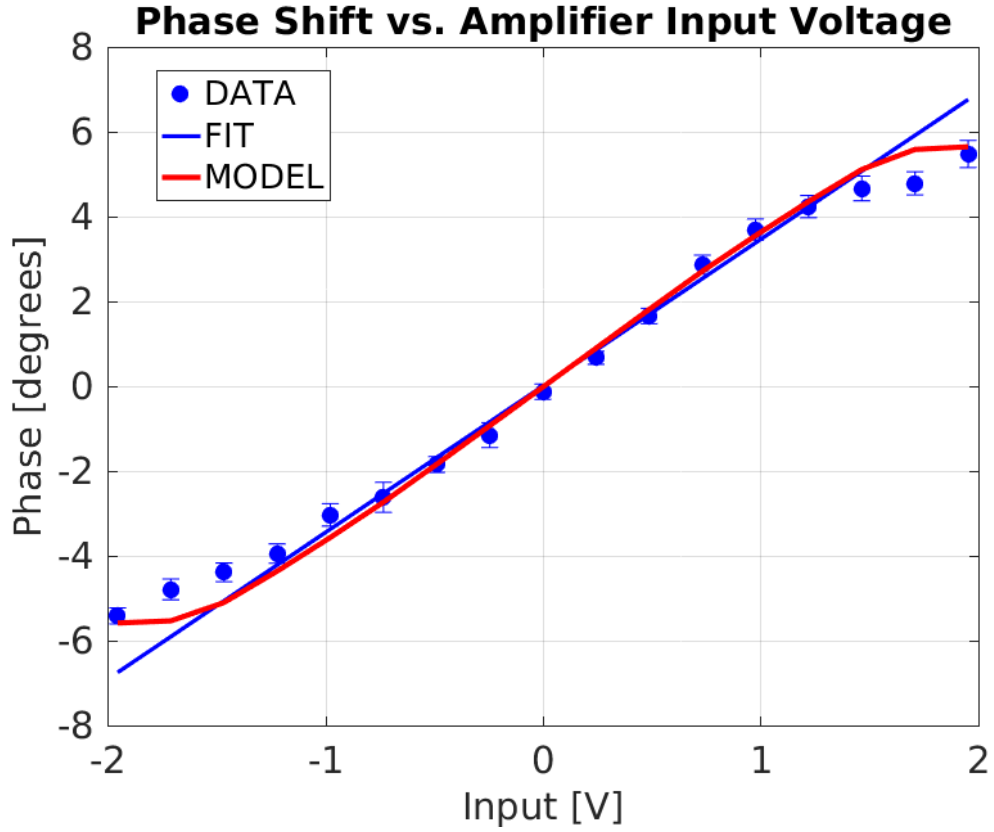
Figure 1.11: Phase shift versus amplifier input voltage.

predicted phase shift, $\Delta\phi$, in degrees is given by:

$$\Delta\phi = V_{amp}[V_{font}].K.R_{52}.\frac{360}{\lambda_{12\text{GHz}}} \tag{1.1}$$

Where $V_{amp}[V_{font}]$ is the amplifier output Voltage at an input voltage of V_{font} sent from the FONT5a board, K is the angular deflection of the beam per Volt applied to each kicker strip, R_{52} is the R_{52} value between the kickers in the PFF optics and $\frac{360}{\lambda_{12\text{GHz}}}$ converts the calculated orbit length difference in to an equivalent 12 GHz phase using the 12 GHz wavelength $\lambda_{12\text{GHz}}$. The value of most of these parameters has already been derived in the sections previously mentioned. They are:

$$V_{amp}[1 \text{ V}] = 435 \text{ V}$$
$$K = 0.8 \ \mu\text{rad/V}$$
$$R_{52} = -0.7 \text{ m}$$
$$\lambda_{12\text{GHz}} = 2.5 \text{ cm}$$

The value of $V_{amp}[1 \text{ V}]$ is given as a representative value in the linear range of the amplifier but the real amplifier output at all input voltages is used in the predictions to include the effects of saturation in the calculated phase shift values. Also, the output sent to the first kicker (from the left side of the amplifier) is used as this is most relevant for the phase shift in the chicane (the orbit should be closed after the second kicker with no further phase shift in the chicane after that point). The value of K is derived from the kicker design, in which
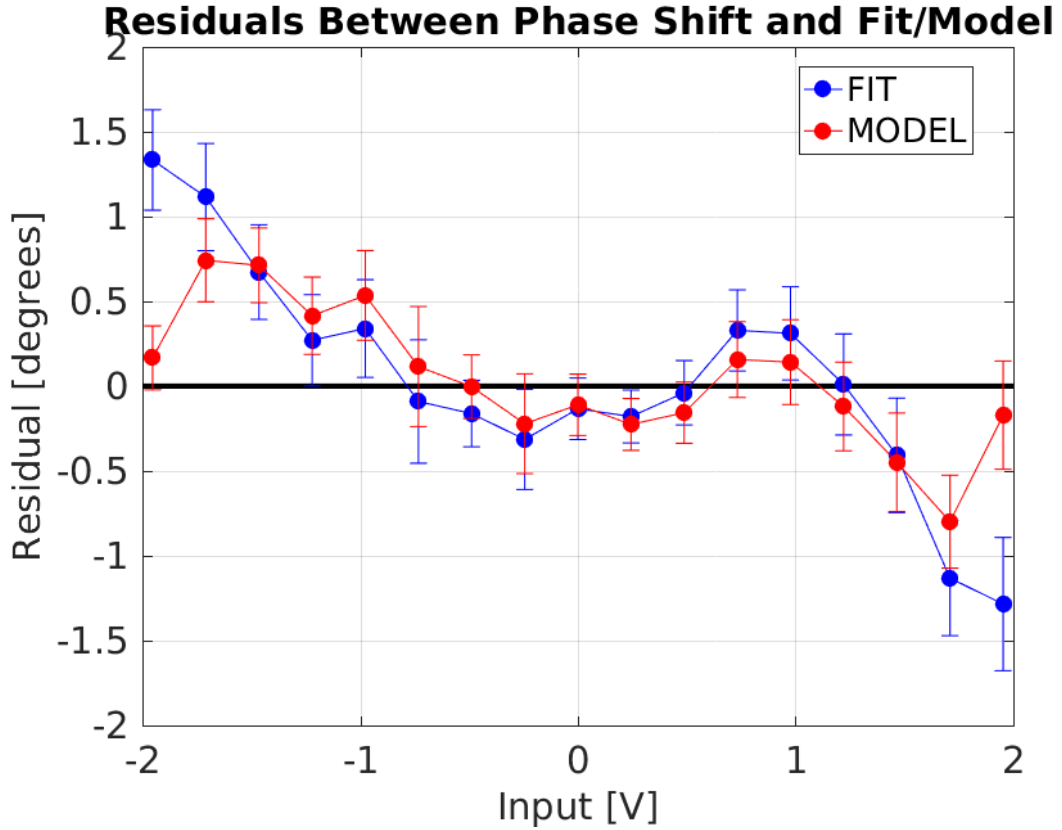
Figure 1.12: Phase shift versus amplifier input voltage.

1.4 kV applied to each strip gives a 1 mrad kick for a 150 MeV beam [TODO: REF]. The actual CTF3 beam energy at this time was approximately 135 MeV (calculated based on the dipole currents used in the machine setup), so the value of K above is scaled by a factor 150/135.

In Figure 1.11 the red line "MODEL" shows the predicted phase shifts using Equation 1.5.1. Table 1.2 compares the fitted gradients and maximum phase shift for the model and real data. The overall agreement between the two is good, with the residuals between both the model and the data, as well as the linear fit to the data and the data, generally consistent with zero within error bars in the ±1.2 V linear range of the amplifier as shown in Figure 1.12.

Outside the linear range some discrepancies appear, although at the maximum ±2 V output the agreement is good so the effect is largest where the amplifier is entering saturation but before hard saturation is reached. However, most amplifier effects can be excluded as the analysis in this section uses the same dataset that was used to characterise the amplifier performance in Section 1.2. This could hint at possible remaining higher order errors in the TL2 chicane optics, or unexpected behaviour from the kickers or amplifier. Although subtracting alternating, interleaved pulses should remove the sensitivity to drifts in the machine it is possible that some residual effect remains. To determine whether the discrepancies are reproducible further scans of this type will need to be completed in the future. The residuals between between the data and the linear fit between ±1.2 V would also

be of significance for the PFF correction should they not converge to zero with additional measurements, as they are of similar magnitude to the 0.2° downstream jitter target.

However, the overall conclusion is as expected — the phase shift in the chicane linearly depends on the amplifier input in the ± 1.2 V (± 2500 DAC counts) region thus a close to optimal correction can be applied in this range, corresponding to a $\pm 4.2 \pm 0.1°$ phase shift. However, when the calculated optimal correction is between an absolute input voltage of 1.2 V and 2.0 V, 2500 to 4096 DAC counts, or $\pm 4.2 \pm 0.1°$ to $\pm 7.0 \pm 0.2°$ the actual phase shift in the chicane is lower, only up to $\pm 5.5 \pm 0.3°$, due to the amplifier entering saturation (and possibly other effects). Any calculated correction outside $\pm 5.5 \pm 0.3°$ receives a static phase shift of $\pm 5.5 \pm 0.3°$ in the chicane. In the limit where all pulses are outside this range the PFF system can only induce a static shift in the mean phase and makes no improvement to the phase jitter. Understanding the impact of the limited correction range on the PFF results was particularly critical for interpreting the early correction attempts with the first version of the amplifier, giving approximately half the ranges shown in this section. This is discussed using simulations of the PFF system in Chapters **??** and **??**.

http://accelconf.web.cern.ch/accelconf/ipac2011/papers/tupc007.pdf 1.4 kV to each strip = 1 mrad kick at 150 MeV 1.26 kV to each strip = 1 mrad kick at 135 MeV

1.5.2   Linearity

1.5.3   Orbit Closure

1.5.4   Shape

Shape of FF kick on BPMs vs. shape of upstream phase

1.6   Correction Output Timing

1.6.1   Absolute Timing

Using Beam Pickup

Using BPMs
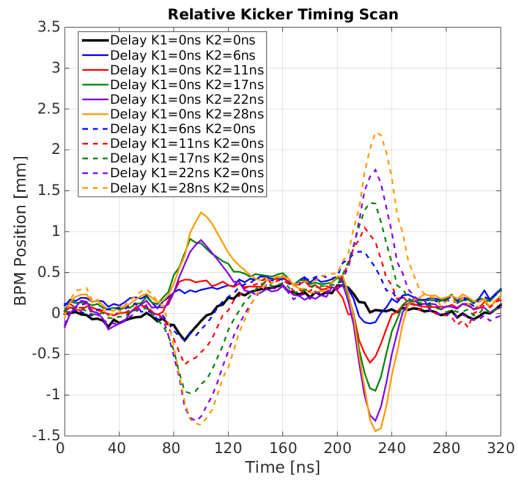
1.6.2   Relative Kicker Timing
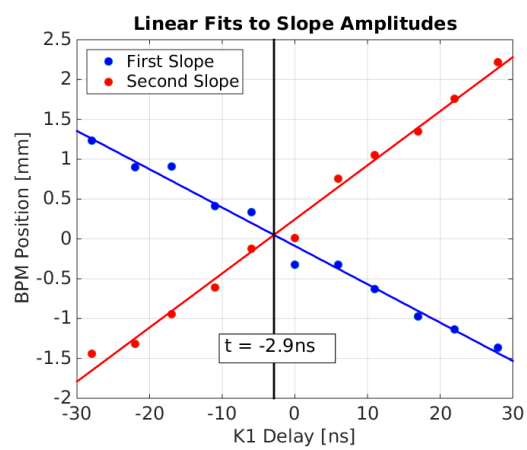
Figure 1.13: Traces relative timing scan.

Figure 1.14: Relative timing scan - fit to rising/falling edge.